molecular pharmaceutics

ACS AuthorChoice

Article

pubs.acs.org/molecularpharmaceutics

Terms of Use

3-D Intestinal Scaffolds for Evaluating the Therapeutic Potential of Probiotics

Cait M. Costello, Rachel M. Sorna, Yih-Lin Goh, Ivana Cengic, Nina K. Jain, and John C. March*

Department of Biological and Environmental Engineering, Cornell University, Ithaca, New York 14853, United States

ABSTRACT: Biomimetic *in vitro* intestinal models are becoming useful tools for studying host−microbial interactions. In the past, these models have typically been limited to simple cultures on 2-D scaffolds or Transwell inserts, but it is widely understood that epithelial cells cultured in 3-D environments exhibit different phenotypes that are more reflective of native tissue, and that different microbial species will preferentially adhere to select locations along the intestinal villi. We used a synthetic 3-D tissue scaffold with villous features that could support the coculture of epithelial cell types with select bacterial populations. Our end goal was to establish microbial niches along the crypt−villus axis in order to mimic the natural microenvironment of the small intestine, which could potentially provide new insights into microbe-induced intestinal disorders, as well as enabling targeted probiotic therapies. We recreated the surface topography of the small intestine by fabricating a biodegradable and biocompatible villous scaffold using poly lactic-glycolic acid to enable the culture of Caco-2 with differentiation along the crypt−villus axis in a similar manner to native intestines. This was then used as a platform to mimic the adhesion and invasion profiles of both *Salmonella* and *Pseudomonas*, and assess the therapeutic potential of *Lactobacillus* and commensal *Escherichia coli* in a 3-D setting. We found that, in a 3-D environment, *Lactobacillus* is more successful at displacing pathogens, whereas Nissle is more effective at inhibiting pathogen adhesion.

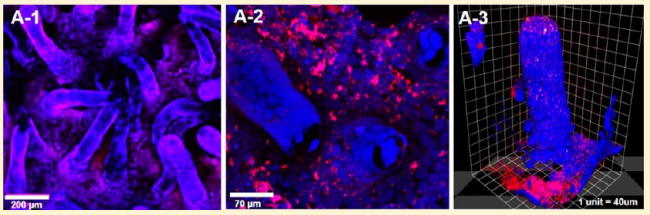

KEYWORDS: *3-D scaffold, intestinal model, probiotics*

1. INTRODUCTION

There is a significant medical need to better understand the interactions of small intestinal epithelial cells with intestinal pathogens, which contribute to and exacerbate a number of diseases including chronic diarrhea,[1,2] gastroenteritis,[3] and necrotizing enterocolitis.[4] The virulent effects of intestinal pathogens are dependent on their ability to colonize and invade the intestinal mucosa, usually by adhering to and penetrating the epithelial layer. Antibiotics have typically been the first line of treatment for intestinal infections, yet with the increasing problem of antibiotic resistance in clinical practice, there has been a need to explore alternative antimicrobial therapies. A potential therapy or prophylactic against microbial pathogenesis is the use of probiotic strains of bacteria, including lactobacilli, bifidobacteria, and commensal *Escherichia coli* (e.g., Nissle 1917), which have been shown in a variety of animal models to confer beneficial effects to the intestinal mucosa by inhibiting pathogen colonization and invasion, and by modulating the host immune response.[5−10] Biomimetic tissue models can provide a rapid and cheap alternative platform to study the interactions of probiotics with intestinal pathogens. At their simplest, these models are typically made up of 2-D confluent monolayers of epithelial cell types, such as Caco-2, HT-29, or HeLa, which are incubated with microbes for short-term monitoring of epithelial−microbe interactions. However, these models do not fully emulate what happens *in vivo*, particularly in regard to the physical three-dimensional space that the cells inhabit, despite it being well-known that bacterial colonization is greatly dependent on their 3-D niche.[11−14] In response, some researchers have developed elegant microfluidic models that create a three-dimensional microenvironment[15,16] and use flow mechanisms to allow simulation of biofilm formation[17] and peristalsis.[18] In addition, the NASA-developed rotating wall vessels (RWV) have enabled prolonged 3-D culture of both mammalian cell types and bacterial populations.[19] This device has been optimized to produce laminar flow to enable the growth of intestinal organoids in suspension culture in conjunction with bacteria to simulate an enteric infection in a fluidic setting. However, thus far the specific three-dimensional surface topography of the intestine has been poorly recreated, i.e., via re-creation of the intestinal villi. Epithelial cells typically become more differentiated and polarized while moving along the crypt−villus axis, and they subsequently express different apical and basolateral receptors. It has been shown *in vitro* by previous researchers that many strains of bacteria will preferentially adhere to epithelial cells in different stages of differentiation. For instance, *Salmonella*, enteropathogenic *E. coli*, and *Listeria* all target receptors such as microvilli on differentiated cells residing on the villi,[20−25] whereas *Yersinia*

Special Issue: Engineered Biomimetic Tissue Platforms for in Vitro Drug Evaluation

Received: February 17, 2014
Revised: May 1, 2014
Accepted: May 5, 2014
Published: May 5, 2014

pseudotuberculosis and *Pseudomonas* have been shown to preferentially adhere to unpolarized, less differentiated cells[26,27] which are found in the crypt regions in real intestines. *Salmonella* has been shown to interact with the microvilli of polarized enterocytes and induce membrane ruffling through cytoskeleton reorganization, allowing them to penetrate the epithelial layer.[20,28] Two of the drawbacks to traditional (2-D) models is that they rarely allow for both undifferentiated and differentiated epithelial cell types to be cultured at the same time and they completely ignore the physical dimensions typical of villus structures. We have previously demonstrated that small sections of synthetic 3-D intestine can be synthesized from collagen,[29,30] silicon,[31] and poly lactic-glycolic acid (PLGA)[32] with realistic villus geometries, which can be used to support the growth and differentiation of epithelial cell types in a manner similar to real intestinal tissue. In this study, we aimed to show that these intestinal models can also be used to evaluate the therapeutic potential of two intestinal probiotics (*Lactobacillus gasseri* and *E. coli* Nissle 1917) against two intestinal pathogens (*Salmonella typhimurium* and *Pseudomonas aeruginosa*) in a more realistic physiological setting. Three scenarios of bacterial adhesion were tested: displacement, competition, and inhibition. Displacement refers to the ability of the probiotic to physically remove an intestinal pathogen after it has established an adhesive niche on the epithelial cells. Competition refers to the ability of the probiotic to compete with the pathogen for adhesive binding sites on the epithelial cells, assuming that the starting inoculum is the same concentration. Inhibition refers to the ability of the probiotic to establish an adhesive niche on the epithelial cells, and then retain this niche it once exposed to pathogen, thereby blocking the pathogen from binding.

2. MATERIALS AND METHODS

2.1. Fabrication of Intestinal Scaffolds. Porous PLGA scaffolds with intestinal villus features were fabricated as described previously.[32] Briefy, micromolding techniques were used to create agarose molds of 500 μm deep, high aspect ratio holes from a poly(methyl methacrylate) (PMMA) template. PLGA (100 mg/mL in chloroform, from Lactel Absorbable Polymers, Birmingham, AL) was mixed with a porogen (sodium bicarbonate, 400 mg/mL) and homogenized for 2 min. Intestinal scaffolds were formed by coating the agarose molds with the PLGA−porogen solution under vacuum, followed by freezing at −20 °C overnight and then immersion in precooled ethanol for 12 h to extract the chloroform. The scaffolds were then immersed in warm distilled water for 24 h to dissolve the porogen, and sterilized with 70% ethanol for 24 h prior to use. Prior to cell seeding, the PLGA scaffolds were placed into a custom designed scaffold-insert kit from previously reported methods,[30] and then soaked overnight in coculture media which was added to both basolateral and apical compartments.

2.2. Cell Culture on Transwell Inserts. Caco-2 cells (ATCC, Manassas, VA) passage 18−25, were expanded and maintained in tissue culture medium [DMEM with 10% fetal bovine serum (FBS), 1× antimycotic−antibiotic, and 1% nonessential amino acids] (all from Invitrogen, Long Island, NY). Cells were maintained in a humidified 37 °C incubator with 5% CO_2, with regular passage 1−2 times a week and medium change every 2 days. Caco-2 were removed from culture flasks with 0.25% (v/v) trypsin, 0.02% EDTA solution in PBS and seeded onto the Transwell insert scaffolds at a concentration of 1×10^5 cells/mL and grown for 21 days, and 1×10^7 cells/mL and cultured for 4 days to produce differentiated and undifferentiated monolayers, respectively. Medium was added to both the basolateral and apical compartments and replaced every 2 days thereafter, and antibiotics were removed from the tissue culture medium the night before bacterial seeding.

2.3. Cell Culture on PLGA Scaffolds. Caco-2 cells were maintained as in section 2.2.Cells were seeded onto the PLGA scaffolds at a concentration of 1×10^7 cells/mL. Medium was added to both the basolateral and apical compartments after a 30 min cell attachment period, and replaced every 2 days thereafter. Experiments were performed at 21 days post Caco-2 seeding to enable cell differentiation along the crypt−villus axis, and antibiotics were removed from the tissue culture medium the night before bacterial seeding.

2.4. Bacterial Strains and Growth Conditions. *Salmonella typhimurium* 14038 (ST), *Pseudomonas aeruginosa* 15692 (PAO1), and *Lactobacillus gasseri* 33323 (LAB) were from ATCC, Manassas, VA. *Escherichia coli* Nissle 1917 (Nissle) was obtained from a commercial preparation of the probiotic Mutaflor as described previously.[33] Overnight cultures of Nissle, ST, and PAO1 were grown in LB medium, and LAB were grown in Difco Lactobacilli MRS medium (all from BD, Franklin Lakes, NJ). Cultures were maintained at 37 °C, with shaking at 225 rpm.

2.5. Bacterial Adhesion Assay on Transwell Inserts. The bacterial adhesion assay was performed as previously described,[34] but with some modifications. A preculture of bacteria was grown for 16 h, before diluting 1:50 in fresh medium and grown back to midexponential phase for a further 1.5 h. Bacteria were then adjusted to a final concentration of 5×10^8 cells/mL in an even mixture of bacterial medium and DMEM (no antibiotics), and 1 mL of bacterial suspension was then added to the apical surface of the Caco-2-covered Transwells, with incubation at 37 °C for 2 h. Nonadhered bacteria were removed by washing twice in PBS, and cells were removed from the scaffolds by incubating with 500 μL of trypsin−EDTA at 37 °C for 10 min. The reaction was blocked with 500 μL of DMEM containing FBS, and serial 10-fold dilutions were plated onto MRS agar for LAB, and MacConkey agar (EMD Millipore, Billerica, MA) for ST, PAO1, and Nissle, with incubation for 24 h at 37 °C. MacConkey agar selects for lactose-fermenting Nissle (pink colonies) against non-lactose-fermenting ST and PAO1 (yellow-brown colonies).

2.6. Bacterial Adhesion Assay on PLGA Scaffolds. The bacterial adhesion assay was performed as in section 2.5, but bacteria were seeded onto the apical surface of PLGA scaffolds in the inset kits, instead of Transwells. The following scenarios of bacterial adhesion were tested: probiotic displacing pathogen (2 h incubation with ST or PAO1 followed by 2 h incubation with Nissle or LAB, at either 1:1 or 3:1 probiotic to pathogen ratios); probiotic inhibiting pathogen adhesion (2 h incubation with Nissle or LAB followed by 2 h incubation with ST or PAO1, at either 1:1 or 3:1 probiotic to pathogen ratios); probiotic competing with pathogen (2 h incubation with mixture of Nissle or LAB and ST or PAO1, at either 1:1 or 3:1 probiotic to pathogen ratios). Adhesion was expressed as $\log^{10}$ CFU/mL.

2.7. Bacterial Invasion Assay. The invasive ability of ST and PAO1 was assessed using the gentamicin protection assay.[34,35] Bacterial adhesion scenarios to the Caco-2 surface were set up as described in section 2.4. Nonadhered bacteria

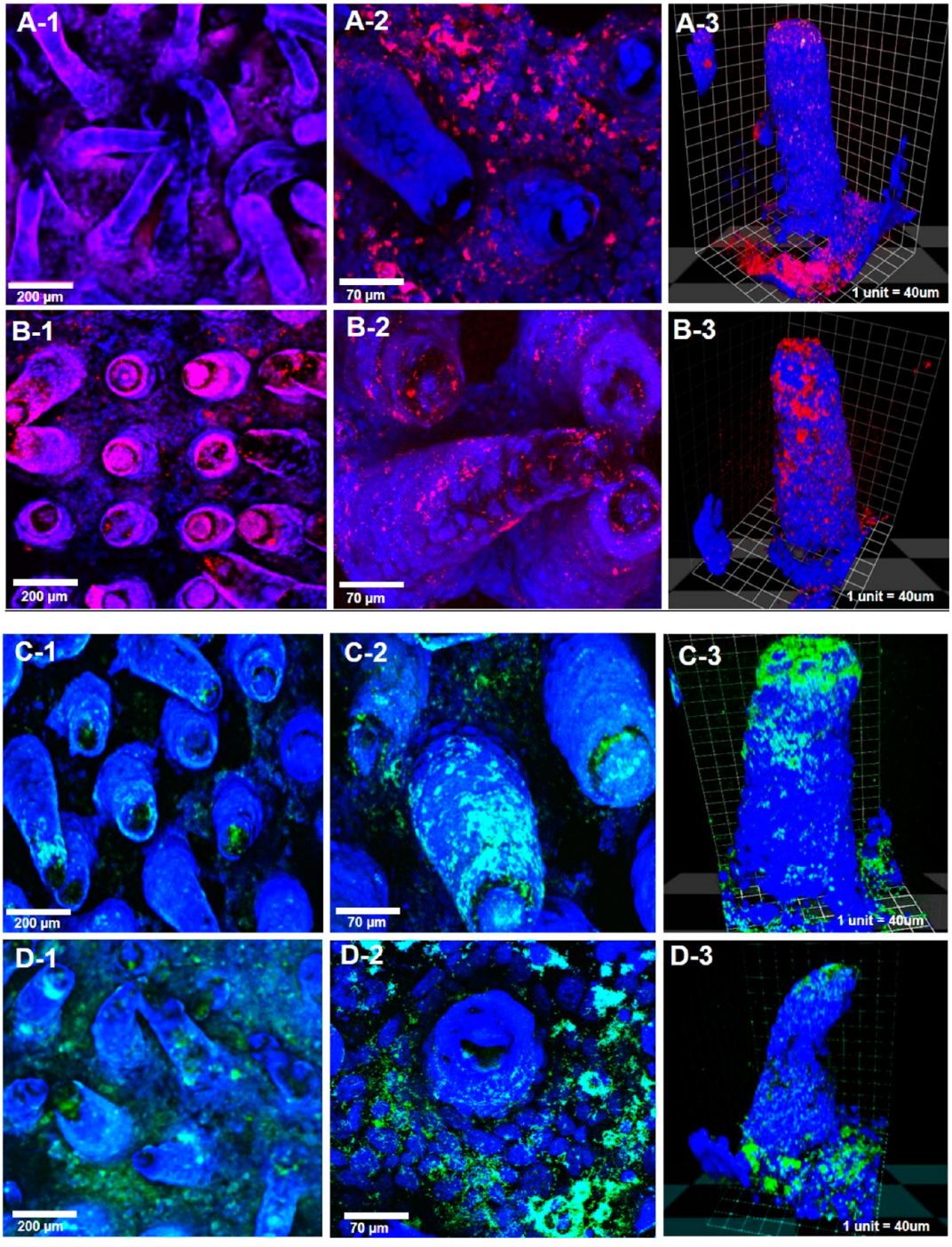

Figure 1. Confocal microscopy of PLGA scaffolds cultured for 21 days with Caco-2 (blue), and 2 h with bacteria (red and green). A = Nissle, B = LAB, C = ST, and D = PAO1. 20× magnification shows full coverage of scaffolds with Caco-2 and bacteria (A-D1) with a zoomed in 40× magnification enabling visualization of individual bacteria (A-D2), and 3-D rendering shows bacteria adhering selectively to different locations along the crypt−villus axis on an individual villus measuring 500 μm (A-D3).

were removed by washing twice in PBS, followed by incubation with 1 mL of gentamicin (150 μg/mL^{-1} in DMEM) for 1 h at 37 °C to kill the adhered extracellular bacteria. Dead bacteria were removed by washing twice in PBS, followed by an incubation with 500 μL of 0.1% Triton X-100 for 15 min at 37 °C to lyse the Caco-2 and release the intracellular (invaded) bacteria. Serial fold dilutions and plating were then employed as described in section 2.4.

2.8. Transepithelial Electrical Resistance (TEER). To measure TEER values of the Caco-2 monolayers before and after bacterial treatments, the medium was aspirated from the insets, replaced with fresh DMEM both basolaterally and apically, and incubated at 37 °C for 15 min. TEER was measured with an EVOM2 epithelial voltohmmeter with STX3 electrodes (World Precision Instruments, Sarasota, FL). Electrodes were placed on the apical and basolateral sides of the inset kits, and the resistance was corrected for surface area (0.5 mm) and expressed as Ω·cm^2. The intrinsic resistance (scaffold) was subtracted from the total resistance (scaffold and Caco-2 cells ± bacteria) to give the monolayer resistance.

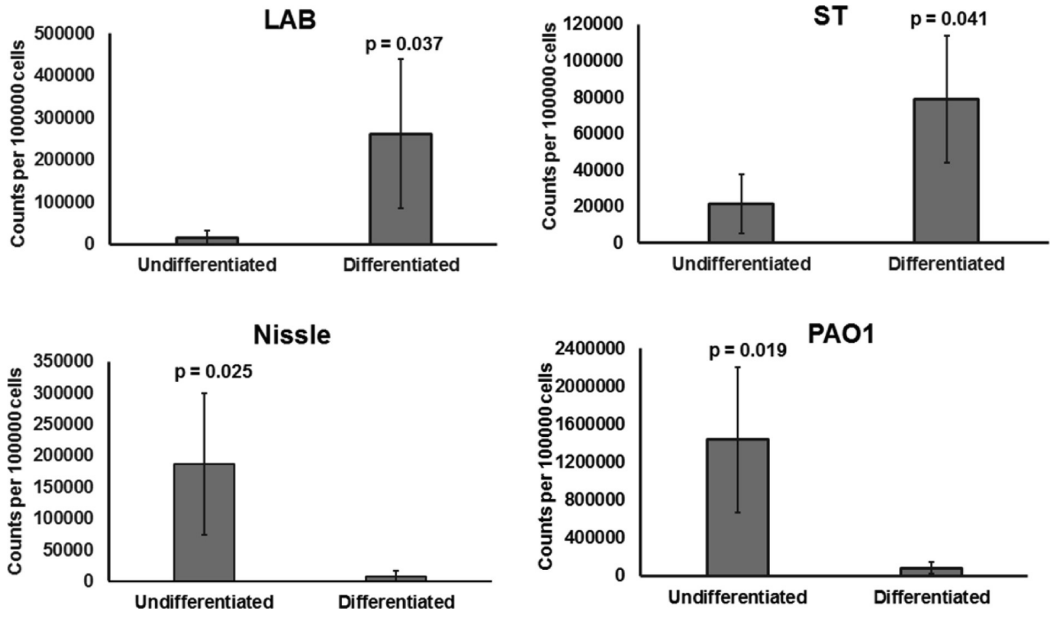

Figure 2. Colony counts from 2-D cultures of Caco-2.

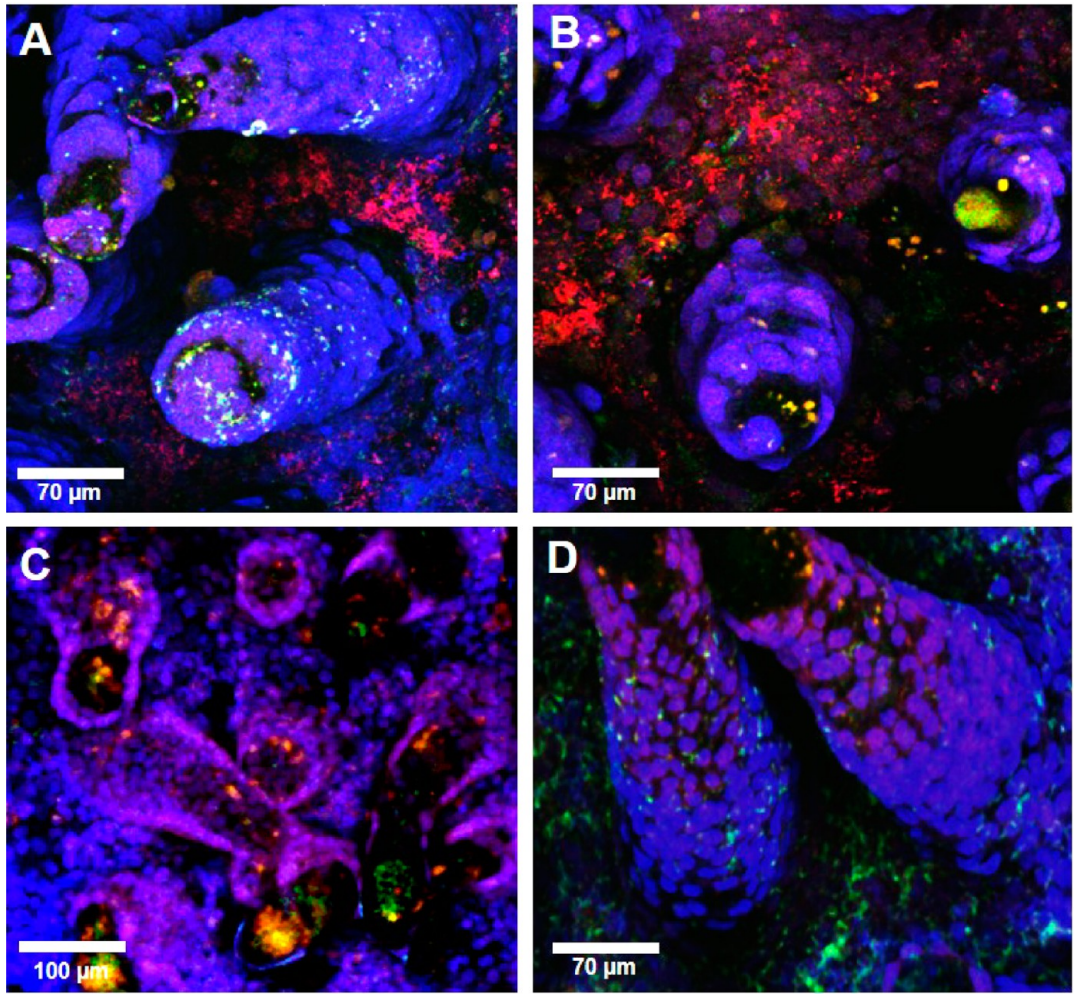

Figure 3. Confocal microscopy of PLGA scaffolds cultured for 21 days with Caco-2 (blue), and 2 h with a 1:1 concentration of probiotic (red) and pathogen (green). A = Nissle and ST, B = Nissle and PAO1, C = LAB and ST, and D = LAB and PAO1.

2.9. MTT Assay. MTT assays were used to assess Caco-2 cell viability in the presence of bacteria using a vybrant MTT assay proliferation kit (Invitrogen) according to the manufacturer's instructions with some modifications. Briefly, bacterial

dx.doi.org/10.1021/mp5001422 | *Mol. Pharmaceutics* 2014, 11, 2030−2039

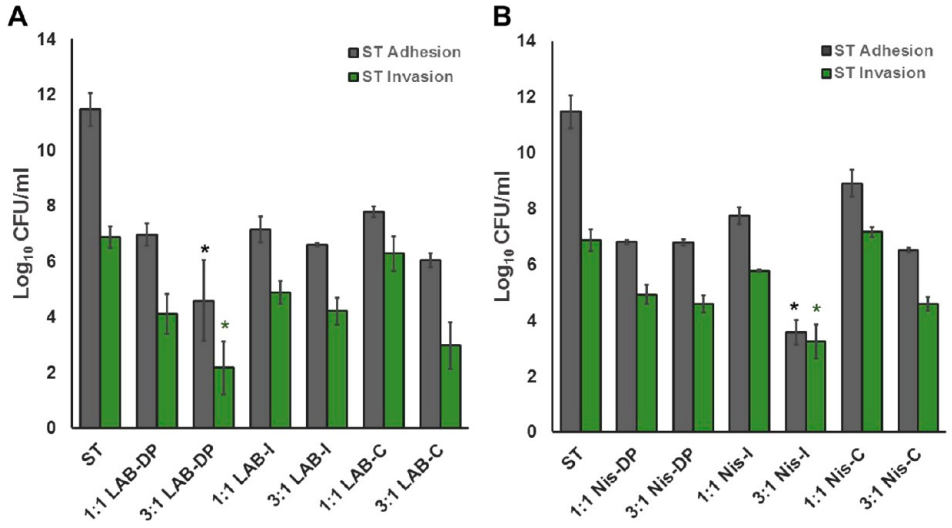

Figure 4. Colony counts from a 2 h incubation of Caco-2 cultures with ST, with results showing adhesion to the Caco-2 surface, or invasion into the Caco-2 cells, expressed as $\log^{10}$ CFU/mL. The colony counts of ST in isolation were compared to colony counts of ST when treated with probiotic LAO1 (A) or Nissle (B); DP = displacement, I = inhibition of adhesion, and C = competition. Significance was assessed with an unpaired *t* test, followed by a Bonferroni correction post test to determine significance across the multiple scenarios ($p < 0.008$). The Bonferroni significances were plotted on the graphs.

adhesion scenarios to the Caco-2 surface were set up as described in section 2.4 and extracellular bacteria were removed with gentamicin as described in section 2.5. After washing twice in PBS, Caco-2 were removed from the scaffold surface by a 10 min incubation with 500 μL of trypsin−EDTA at 37 °C. Cells were centrifuged for 5 min at 150*g*, resuspended in DMEM, and adjusted to a cell density of 1×10^5 cells/mL. A 100 μL suspension of each cell sample was added to a 96 well plate and incubated for 36 h at 37 °C with 5% CO_2. The wells were replaced with fresh medium containing 10 μL of 12 mM MTT stock solution and incubated for 4 h at 37 °C, followed by incubation with 100 μL of SDS−HCl solution for a further 4 h. The absorbance was read at 570 nm, and cell viability was assessed against control samples of intestinal scaffolds that had not been exposed to bacteria, and expressed as % cell survival.

2.10. FISH and Confocal Imaging. Fluorescence *in situ* hybridization (FISH) enabled visualization of the adherent bacteria on the Caco-2 monolayers, using the following probes: TTT CAT CTG GTG CAA GCA CC (LAB); TCT CGG CCT TGA AAC CCC (PAO1) AAT CAC TTC ACC TAC GTG (ST); TT-FISH-CAC CGT AGT GCC TCG TCA (Nissle). Intestinal cell-coated PLGA scaffolds were fixed with 4% paraformaldehyde for 20 min at room temperature, then dehydrated by submerging in 50% ethanol for 3 min, 80% ethanol for 3 min, and then 100% ethanol for 3 min. Samples were incubated overnight in a humidified chamber at 45 °C in hybridization buffer (0.01% SDS, 20 mM Tris-HCL, 900 mM NaCl, and 30% formamide in PBS) containing 5 ng/μL FISH probe. Samples were then incubated at 45 °C for 25 min with washing buffer (450 mM NaCl, 20 mM Tris, 5 mM EDTA, and 0.01% SDS in dH_2O), followed by a further two washes to remove nonspecific binding of the probe. Caco-2 nuclei were counterstained with TO-PRO-3 (Invitrogen). Samples were scanned using a Leica SP2 confocal microscope (Leica Microsystems, Buffalo Grove, IL) with Z-series capability. Three-dimensional rendering images and sections were assembled with Volocity 5.0 software (PerkinElmer, Waltham, MA) and ImageJ.

2.11. Statistical Analysis. TEER, all cell counts, and MTT assays were performed in triplicate, and data are presented as means ± SD. Statistical differences were determined by using a Student's unpaired *t* test, with *p* values of less than 0.05 being considered significant ($\alpha = 0.05$). For experiments in which we had 12 scenarios of adhesion we used a Bonferroni correction and divided α by 12 and hence regarded *p* values of less than 0.004 as statistically significant. We also used a Bonferroni correction on plate counts; however, in this scenario, since we separated the probiotics into 2 separate experiments that looked at both adhesion and invasion, we divided α by 6.

3. RESULTS

3.1. Adhesion and Location of Bacteria on Intestinal PLGA Scaffolds. FISH and confocal microscopy was used to determine the location of the four strains of bacteria to the Caco-2 monolayers on intestinal PLGA scaffolds (Figure 1). The images show a clear difference in adhesive niche along the crypt−villus axis between the strains of bacteria. The majority of the Nissle (Figure 1A) and PAO1 (Figure1C) cells located to the base of the scaffold where the undifferentiated cells resided, whereas most of the LAB and ST and primarily located to the tips of the villi, on the differentiated cells. Figure 2 shows colony counts from 2-D cultures of Caco-2 (no villi), cultured on polyester Transwell inserts for 4 days and 21 days, which produce undifferentiated and differentiated monolayers, respectively. Differentiation states were verified by TEER as described previously.[32] Colony counts were normalized to Caco-2 cell number to account for differences in cell density in the two data sets. For both LAB and ST, the highest number of cells adhered to the 21 day differentiated Caco-2 cultures, and for both Nissle and PAO1 the highest counts were on the 4 day undifferentiated cultures. Figure 3 shows the location of the bacteria on the intestinal scaffolds when used in a 1:1 pathogen/probiotic ratio. The images show that Nissle and ST have a different adhesive niche (Figure 3A), compared to Nissle and PAO1, which share a similar adhesive niche in the crypt region (Figure 3B). In contrast, LAB and ST are located in similar positions with the differentiated cells on the villus

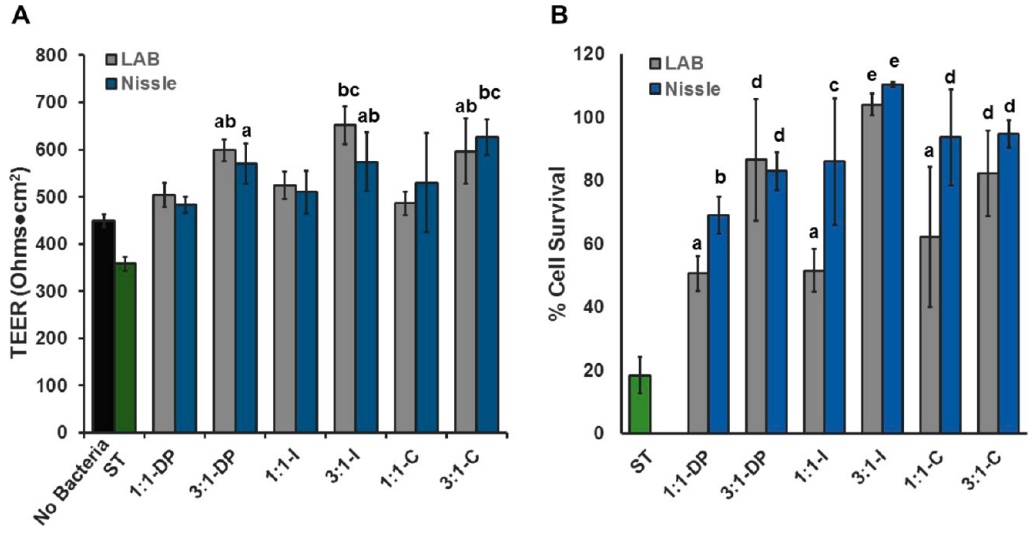

Figure 5. TEER values (A) and % cell survival from MTT assay (B) of Caco-2 monolayer PLGA scaffolds after incubation for 2 h with the pathogen ST, and then a series of treatments with a 3:1 or 1:1 ratio of probiotic LAB or Nissle. DP = displacement, I = inhibition of adhesion, and C = competition. Significance was assessed by comparing TEER and % cell survival to samples with pathogen only (no probiotic) using an unpaired *t* test, followed by a Bonferroni correction post test to determine significance across the multiple scenarios ($p < 0.004$). The Bonferroni significances were plotted on the graphs (a−e = lowest to highest significance).

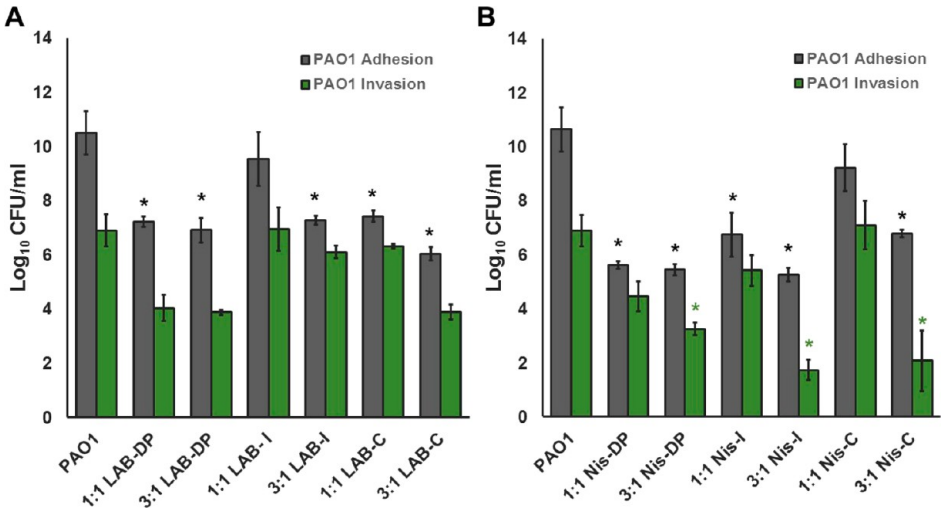

Figure 6. Colony counts from a 2 h incubation of Caco-2 cultures PAO1, with results showing adhesion to the Caco-2 surface, or invasion into the Caco-2 cells, expressed as $\log^{10}$ CFU/mL. The colony counts of PAO1 in isolation were compared to colony counts of ST when treated with probiotic LAO1 (A) or Nissle (B); DP = displacement, I = inhibition of adhesion, and C = competition. Significance was assessed with an unpaired *t* test, followed by a Bonferroni correction post test to determine significance across the multiple scenarios ($p < 0.008$).

(Figure 3C), whereas the majority of LAB and PAO1 were in different positions.

3.2. Protective Effects of Probiotics against Adhesion and Invasion of ST. The adhesive and invasive activity of ST and the potential therapeutic effects of the probiotics were assessed through colony counts for adhesion and invasion, measurements of tight junction integrity through TEER, and Caco-2 cell survival using an MTT assay. The probiotics were assessed for their ability to displace ST from the scaffolds, inhibit the adhesion of ST, or compete with the pathogen for colonization space, as well as how these scenarios affected the invasion of ST into the Caco-2 cells. Figure 4A shows that LAB reduced the adhesion of ST to the Caco-2 through displacement, inhibition, and competition. Reduction in adhesion through displacement and competition appeared to be a dose-dependent event, with a greater reduction being obtained by using a 3:1 ratio of LAB to ST. Using the Bonferroni post test it was found that, with a 3:1 ratio of LAB to ST, a significant reduction of ST adhesion occurred via displacement. A 3:1 ratio of LAB used in the displacement assay also gave the greatest reduction in invasion into the Caco-2 monolayers. Similarly, the reduction of ST using Nissle as the probiotic appeared to be a dose-related event, and none of the 1:1 adhesion scenarios were significant. However, in contrast to LAB, which was most effective at displacing ST, Nissle was most effective against ST when used as a high-dose pretreatment to inhibit adhesion.

Figure 5A shows that, in isolation, ST reduces the TEER of Caco-2 monolayers compared to a bacteria-free control. Both LAB and Nissle increased TEER values for Caco-2 cells growing on the scaffolds in a dose-dependent manner, despite the presence of ST. This increase was significant for all three scenarios of adhesion with a 3:1 ratio of probiotic to pathogen.

dx.doi.org/10.1021/mp5001422 | *Mol. Pharmaceutics* 2014, 11, 2030−2039

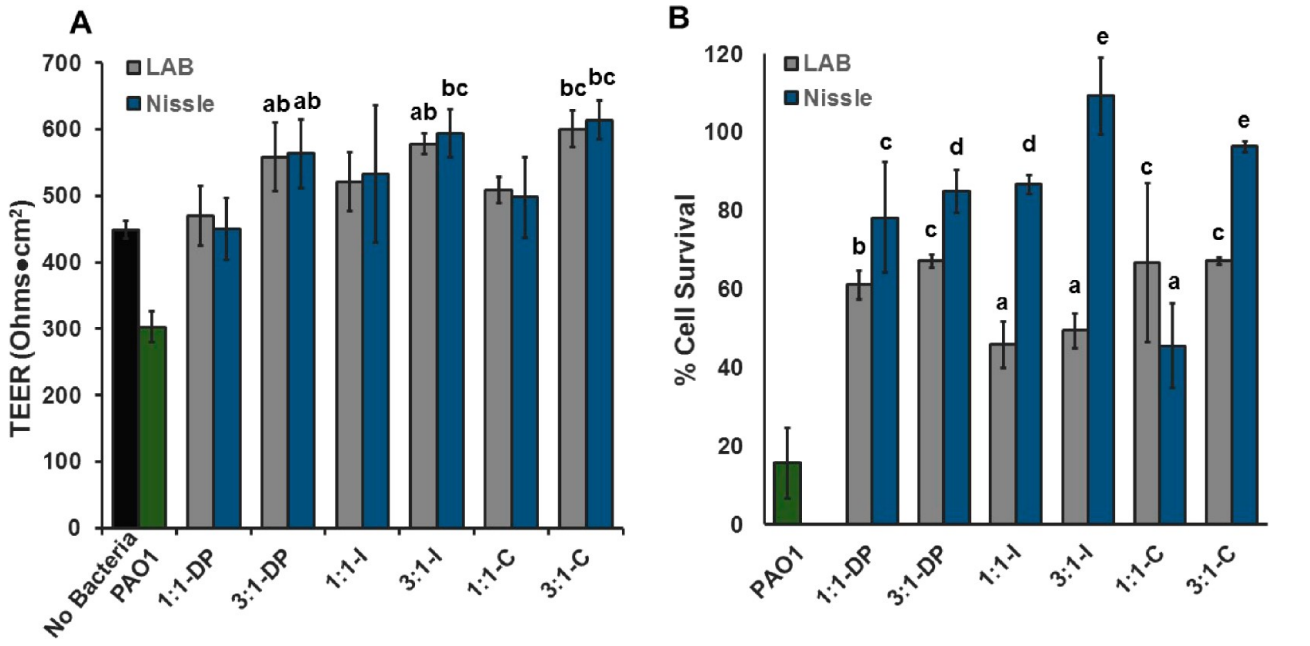

Figure 7. TEER values (A) and % cell survival from MTT assay (B) of Caco-2 monolayer PLGA scaffolds after incubation for 2 h with the pathogen PAO1, and then a series of treatments with 3:1 or 1:1 ratio of probiotic LAB or Nissle. DP = displacement, I = inhibition of adhesion, and C = competition. Significance was assessed by comparing TEER and % cell survival to samples with pathogen only (no probiotic) using an unpaired *t* test, followed by a Bonferroni correction post test to determine significance across the multiple scenarios ($p < 0.004$). The Bonferroni significances were plotted on the graphs (a–e = lowest to highest significance).

In addition, the percentage cell survival significantly increased with the addition of LAB and Nissle (Figure 5B). Applying a 3× probiotic treatment to the Caco-2 before the addition of ST promoted the highest level of cell survival, with no difference to control samples without ST (i.e, 100% cell survival). The displacement and competition scenarios at a 3:1 ratio enabled over 80% of the cells to survive, with no significant difference between the two. Nissle appeared to promote higher levels of cell survival compared to LAB at lower concentrations (1:1) however, with a significant difference in all three scenarios tested.

3.3. Protective Effects of Probiotics against Adhesion and Invasion of PAO1. The adhesive and invasive potential of PAO1 and the subsequent therapeutic effects of the probiotics were assessed using colony counts, TEER, and an MTT assay. It was found that LAB significantly lowered the number of adhered ST to the Caco-2 in all scenarios tested except the 1:1 inhibition assay (Figure 6A). Invasion was not significantly reduced in any case, even with higher dose of LAB. It was found that Nissle significantly lowered the number of adhered ST to the apical surface of the Caco-2 in most scenarios tested, except the 1:1 competition assay. In contrast to LAB, Nissle managed to significantly reduce invasion into the Caco-2 cells in every scenario with a high dose of probiotic (Figure 6B).

As with the pathogen ST, Figure 7A shows that, in isolation, PAO1 reduced the TEER of Caco-2 monolayers compared to a bacteria-free control, and that both probiotics raised TEER values when used in conjunction with PAO1. Again, the rise in TEER was dose-dependent: higher concentrations of probiotic had a more significant effect across all scenarios tested. Displacement and competition treatments raised the TEER more than inhibition, however, there was little difference between the two strains of probiotic. However, there was a difference in how the two probiotics affected cell survival. Although the percentage cell survival was significantly improved in all scenarios tested, treatments with Nissle fared better than LAB in all cases except a 1:1 competition (Figure 7B).

4. DISCUSSION

Biomimetic tissue cell models can be used to simplify studies on bacterial–host cell interactions to determine the effects of one or two specific factors. In this study, we looked at the effects of intestinal epithelial cell differentiation on the adhesion and invasion of two pathogens, and the subsequent potentially therapeutic or prophylactic effects of two well-known probiotics. It has been shown extensively in the literature that the differentiation of Caco-2 is a growth related process that closely mimics the differentiation profiles of small intestinal epithelium *in vivo*,[36−39] with undifferentiated cells during exponential growth that turn into polarized and differentiated cells at postconfluence. In the small intestine, this process occurs along the crypt–villus axis, with dividing nondifferentiated cells residing near the crypt regions that move up the villi to become more differentiated cells. We have shown in our previous studies that we can mimic this phenomenon using a 3-D villus scaffold to support the directional growth and differentiation of Caco-2.[29,30,32] Nondifferentiated intestinal epithelial cells express basolateral markers over the entire surface (including cadherins, integrins, etc.) whereas differentiated epithelial cells also display apical markers, including brush border enzymes and microvilli. It has been shown in previous *in vivo* studies that certain strains of bacteria will preferentially adhere to epithelial cells in different stages of differentiation. The pathogen *Salmonella* has been shown to interact with the apical surface of differentiated epithelial cells in the intestine, which is accompanied by a degeneration of microvilli upon invasion.[20,21,35] In contrast, some strains of *Pseudomonas* including PAO1 may preferentially adhere to and invade nondifferentiated cells.[40] Also, through wound-healing experiments, it

dx.doi.org/10.1021/mp5001422 | *Mol. Pharmaceutics* 2014, 11, 2030–2039

was shown that higher levels of *Pseudomonas* interact with cells that had reverted back to their nondifferentiated state.[27,41] It has been suggested that *Pseudomonas* may preferentially interact with basolateral receptors, although it is worth noting that this phenomenon has not been as widely characterized as *Salmonella*. We have shown that, using both traditional 2-D Transwell inserts and our biomimetic model, the ecological niche of both ST and PAO1 resembles that of previously reported methods, with the majority of adhesion at differentiated cells at the tips of the villi and undifferentiated cells near the crypt region, respectively. In addition, the higher levels of LAB adhesion to the differentiated cells at the tips of the villi were in agreement with the literature.[42] Some strains of *E. coli* have been found to interact mainly with differentiated cell types;[43] however, in our 3-D model we found that the majority of Nissle was located near the undifferentiated cells at the base of the villi, and this could potentially be due to the variation in adhesins expressed by different strains of *E. coli* (Nissle for example has no S-fimbriae and inactive P-fimbriae[44]). As a further demonstration of the different bacterial niches in the small intestine, we also showed that two strains of bacteria could be cultured in a 3-D model in different locations along the crypt−villus axis. Our hypothesis was that the therapeutic potential of probiotics against intestinal pathogens may be altered based on the differences in ecological niche.

In our 3-D intestinal model, we found that both probiotics tested successfully reduced the adhesion and invasion of ST into Caco-2 monolayers in a dose-dependent manner, in good agreement with the literature, which has shown extensively that LAB[45−49] and Nissle[50−53] can be used to displace, compete with, and inhibit ST adhesion and invasion. Further, we found that probiotics were most effective at different stages of ST infection. Although both treatments worked, LAB appeared to be more successful at displacing the pathogen once it had already adhered to the Caco-2 cells as opposed to inhibiting ST adhesion through a preincubation. In contrast, with Nissle the opposite was true, which was surprising as we predicted that the location of Nissle in the crypt regions may reduce the likelihood of ST inhibition as they were shown to have different adhesive niche, but this suggests that factors other than steric hindrance play a role in its therapeutic effects. The colony counts were supported by results from an MTT assay, which showed that cell survival after incubation with ST was highest after a 2 h preincubation with Nissle.

As well as having therapeutic affects against ST, strains of *Lactobacillus* have also been shown by previous researchers to display antimicrobial activity against enteroinvasive *Pseudomonas* strains *in vitro*,[54,55] and we have shown in this study that, in a 3-D setting, even though LAB and PAO1 occupy a different adhesive niche along the crypt−villus axis, the probiotic is still able to inhibit the adhesion of PAO1 to the apical surface of the cells. This shows that, in the same way as Nissle with ST, steric hindrance is not essential to the antimicrobial activity of the probiotic. There is very little in the literature regarding the use of Nissle to treat a *Pseudomonas* intestinal infection, although there is some evidence that it can be used to treat urinary tract infections from *Pseudomonas* through bactericidal activity.[56] Our results suggest that Nissle can be used to effectively lower the adhesion and invasion of PAO1 into epithelial cells in a dose-dependent manner, particularly through inhibition and displacement. Interestingly, Nissle was the only probiotic that significantly prevented the invasion of PAO1 into the Caco-2 cells, as well as promoting greater Caco-2 cell survival for an infection with PAO1 over LAB across all scenarios of adhesion tested, apart from a 1:1 competition scenario. This could therefore potentially be used as a preferred method of probiotic treatment.

5. CONCLUSIONS

We have demonstrated the feasibility of developing an *in vitro* artificial intestine from a biocompatible polymer, which can be molded into villous shapes to mimic the topography of the small intestine, providing a platform for the differentiation of epithelial cell types, and the subsequent adhesion/invasion of pathogenic bacteria. We showed that strains of bacteria can live on epithelial cells that are in different stages of differentiation, and that this alters where they reside on the crypt−villus axis. We showed that, in this 3-D environment, probiotics exert their effects through different mechanisms. For example, LAB was more effective at displaying pathogenic bacteria once it had colonized, and Nissle was more effective at preventing attachment. With further experimentation, we believe that this system could provide a platform for more specific targeting of probiotics to certain intestinal pathogens, for example to determine which probiotics are best to be taken routinely as an inhibitory measure, and which can be used for elimination of an infection once established.

AUTHOR INFORMATION

Corresponding Author

*Tel: +1-607-254-5471. Fax: +1-607-255-4449. E-mail: jcm224@cornell.edu.

Notes

The authors declare no competing financial interest.

ACKNOWLEDGMENTS

We are grateful to the Wiedmann lab (Food Science, Cornell) and the Angenant lab (Biological and Environmental Engineering, Cornell) for donating the *Salmonella* and *Pseudomonas* strains, respectively. We thank the fine mechanics workshop, Chemical Engineering, Cornell, for constructing the tissue culture inserts. We thank Carol Bayes for support with confocal microscopy at the Weill Hall imaging facilities, Cornell. Also, we acknowledge The Hartwell Foundation (Collaborative Award to J.C.M.), the Defense Threat Reduction Agency (DTRA) (Grant HDTRA1-13-1-0037), and the NIH (Grant 1DP2OD007155-01 to J.C.M.).

REFERENCES

(1) Moon, H. W. Mechanisms in pathogenesis of diarrhea - review. *J. Am. Vet. Med. Assoc.* **1978**, *172* (4), 443−448.

(2) Navaneethan, U.; Giannella, R. A. Mechanisms of infectious diarrhea. *Nat. Clin. Pract. Gastroenterol. Hepatol.* **2008**, *5* (11), 637−647.

(3) Mead, P. S.; Slutsker, L.; Dietz, V.; McCaig, L. F.; Bresee, J. S.; Shapiro, C.; Griffin, P. M.; Tauxe, R. V. Food-related illness and death in the United States. *Emerging Infect. Dis.* **1999**, *5* (5), 607−625.

(4) Palmer, C.; Bik, E. M.; DiGiulio, D. B.; Relman, D. A.; Brown, P. O. Development of the human infant intestinal microbiota. *PLoS Biol.* **2007**, *5* (7), 1556−1573.

(5) Madsen, K.; Cornish, A.; Soper, P.; McKaigney, C.; Jijon, H.; Yachimec, C.; Doyle, J.; Jewell, L.; De Simone, C. Probiotic bacteria enhance murine and human intestinal epithelial barrier function. *Gastroenterology* **2001**, *121* (3), 580−591.

(6) Huang, Y.; Adams, M. C. An in vitro model for investigating intestinal adhesion of potential dairy propionibacteria probiotic strains using cell line C2BBe1. *Lett. Appl. Microbiol.* **2003**, *36* (4), 213−216.

(7) Servin, A. L.; Coconnier, M. H. Adhesion of probiotic strains to the intestinal mucosa and interaction with pathogens. *Best Pract. Res. Clin. Gastroenterol.* **2003**, *17* (5), 741−754.
(8) Sartor, R. B. Probiotic therapy of intestinal inflammation and infections. *Curr. Opin. Gastroenterol.* **2005**, *21* (1), 44−50.
(9) Sanchez, B.; Urdaci, M. C.; Margolles, A. Extracellular proteins secreted by probiotic bacteria as mediators of effects that promote mucosa-bacteria interactions. *Microbiology* **2010**, *156* (Part 11), 3232−3242.
(10) Bernardo, D.; Sanchez, B.; Al-Hassi, H. O.; Mann, E. R.; Urdaci, M. C.; Knight, S. C.; Margolles, A. Microbiota/Host Crosstalk Biomarkers: Regulatory Response of Human Intestinal Dendritic Cells Exposed to Lactobacillus Extracellular Encrypted Peptide. *PLoS One* **2012**, *7* (5), e36262.
(11) Shanahan, F. The host-microbe interface within the gut. *Best Pract. Res. Clin. Gastroenterol.* **2002**, *16* (6), 915−931.
(12) Nickerson, C. A.; Richter, E. G.; Ott, C. M. Studying host-pathogen interactions in 3-D: Organotypic models for infectious disease and drug development. *J. Neuroimmune Pharmacol.* **2007**, *2* (1), 26−31.
(13) Marzorati, M.; Van den Abbeele, P.; Possemiers, S.; Benner, J.; Verstraete, W.; Van de Wiele, T. Studying the host-microbiota interaction in the human gastrointestinal tract: basic concepts and in vitro approaches. *Ann. Microbiol.* **2011**, *61* (4), 709−715.
(14) Roeselers, G.; Ponomarenko, M.; Lukovac, S.; Wortelboer, H. M. Ex vivo systems to study host-microbiota interactions in the gastrointestinal tract. *Best Pract. Res. Clin. Gastroenterol.* **2013**, *27* (1), 101−113.
(15) Pfluger, C. A.; McMahon, B. J.; Carrier, R. L.; Burkey, D. D. Precise, biomimetic replication of the multiscale structure of intestinal basement membrane using chemical vapor deposition. *Tissue Eng., Part A* **2013**, *19* (5−6), 649−656.
(16) Wang, L.; Murthy, S. K.; Fowle, W. H.; Barabino, G. A.; Carrier, R. L. Influence of micro-well biomimetic topography on intestinal epithelial Caco-2 cell phenotype. *Biomaterials* **2009**, *30* (36), 6825−6834.
(17) Kim, J.; Hegde, M.; Jayaraman, A. Co-culture of epithelial cells and bacteria for investigating host-pathogen interactions. *Lab Chip* **2010**, *10* (1), 43−50.
(18) Kim, H. J.; Huh, D.; Hamilton, G.; Ingber, D. Human gut-on-a-chip inhabited by microbial flora that experiences intestinal peristalsis-like motions and flow. *Lab Chip* **2012**, *12*, 2165−2174.
(19) Barrila, J.; Radtke, A. L.; Crabbe, A.; Sarker, S. F.; Herbst-Kralovetz, M. M.; Ott, C. M.; Nickerson, C. A. Organotypic 3D cell culture models: using the rotating wall vessel to study host-pathogen interactions. *Nat. Rev. Microbiol.* **2010**, *8* (11), 791−801.
(20) Finlay, B. B.; Falkow, S. Salmonella interactions with polarized human intestinal Caco-2 epithelial-cells. *J. Infect. Dis.* **1990**, *162* (5), 1096−1106.
(21) Giannasca, K. T.; Giannasca, P. J.; Neutra, M. R. Adherence of Salmonella typhimurium to Caco-2 cells: Identification of a glycoconjugate receptor. *Infect. Immun.* **1996**, *64* (1), 135−145.
(22) Shah, D. H.; Zhou, X.; Addwebi, T.; Davis, M. A.; Call, D. R. In vitro and in vivo pathogenicity of Salmonella enteritidis clinical strains isolated from North America. *Arch. Microbiol.* **2011**, *193* (11), 811−821.
(23) Gaillard, J. L.; Finlay, B. B. Effect of cell polarization and differentiation on entry of Listeria monocytogenes into the enterocyte-like Caco-2 cell line. *Infect. Immun.* **1996**, *64* (4), 1299−1308.
(24) Carvalho, H. M.; Teel, L. D.; Goping, G.; O'Brien, A. D. A three-dimensional tissue culture model for the study of attach and efface lesion formation by enteropathogenic and enterohaemorrhagic Escherichia coli. *Cellular Microbiology* **2005**, *7* (12), 1771−1781.
(25) Gabastou, J. M.; Kerneis, S.; Bernetcamard, M. F.; Barbat, A.; Coconnier, M. H.; Kaper, J. B.; Servin, A. L. Two stages of enteropathogenic Escherichia coli intestinal pathogenicity are up and down-regulated by the epithelial cell differentiation. *Differentiation* **1995**, *59* (2), 127−134.
(26) Coconnier, M. H.; Bernetcamard, M. F.; Servin, A. L. How intestinal epithelial cell differentiation inhibits the cell-entry of Yersinia pseudotuberculosis in colon carcinoma Caco-2 cell line in culture. *Differentiation* **1994**, *58* (1), 87−94.
(27) Pereira, S. H. M.; Cervante, M. P.; deBentzmann, S.; Plotkowski, M. C. Pseudomonas aeruginosa entry into Caco-2 cells is enhanced in repairing wounded monolayers. *Microb. Pathog.* **1997**, *23* (4), 249−255.
(28) Finlay, B. B.; Ruschkowski, S.; Dedhar, S. Cytoskeletal rearrangements accompanying Salmonella entry into epithelial cells. *J. Cell Sci.* **1991**, *99*, 283−296.
(29) Sung, J. H.; Yu, J.; Luo, D.; Shuler, M. L.; March, J. C. Microscale 3-D hydrogel scaffold for biomimetic gastrointestinal (GI) tract model. *Lab Chip* **2011**, *11* (3), 389−392.
(30) Yu, J.; Peng, S.; Luo, D.; March, J. C. In vitro 3D human small intestinal villous model for drug permeability determination. *Biotechnol. Bioeng.* **2012**, *109* (9), 2173−2178.
(31) Esch, M. B.; Sung, J. H.; Yang, J.; Yu, C.; Yu, J.; March, J. C.; Shuler, M. L. On chip porous polymer membranes for integration of gastrointestinal tract epithelium with microfluidic 'body-on-a-chip' devices. *Biomed. Microdevices* **2012**, *14* (5), 895−906.
(32) Costello, C. M.; Hongpeng, J.; Shaffiey, S.; Yu, J.; Jain, N. K.; Hackam, D.; March, J. C. Synthetic Small Intestinal Scaffolds for Improved Studies of Intestinal Differentiation. *Biotechnol. Bioeng.* **2014**, *111* (6), 1222−1232.
(33) Duan, F.; March, J. C. Interrupting Vibrio cholerae infection of human epithelial cells with engineered commensal bacterial signaling. *Biotechnol. Bioeng.* **2008**, *101* (1), 128−134.
(34) Gagnon, M.; Berner, A. Z.; Chervet, N.; Chassard, C.; Lacroix, C. Comparison of the Caco-2, HT-29 and the mucus-secreting HT29-MTX intestinal cell models to investigate Salmonella adhesion and invasion. *J. Microbiol. Methods* **2013**, *94* (3), 274−279.
(35) Steele-Mortimer, O. Infection of epithelial cells with Salmonella enterica. *Methods Mol. Biol.* **2008**, *431*, 201−211.
(36) Pinto, M.; Robineleon, S.; Appay, M. D.; Kedinger, M.; Triadou, N.; Dussaulx, E.; Lacroix, B.; Simonassmann, P.; Haffen, K.; Fogh, J.; Zweibaum, A. Enterocyte-like differentiation and polarization of the human colon carcinoma cell line Caco-2 in culture. *Biol. Cell* **1983**, *47*, 323−330.
(37) Jumarie, C.; Malo, C. Caco-2 cells cultured in serum-free medium as a model for the study of enterocytic differentiation in vitro. *J. Cell. Physiol.* **1991**, *149* (1), 24−33.
(38) Basson, M. D.; Turowski, G.; Emenaker, N. J. Regulation of human (Caco-2) intestinal epithelial cell differentiation by extracellular matrix proteins. *Exp. Cell Res.* **1996**, *225* (2), 301−305.
(39) Simon-Assman, P.; Turck, N.; Sidhoum-Jenny, M.; Gradwohl, G.; Kedinger, M. In vitro models of intestinal epithelial cell differentiation. *Cell Biol. Toxicol.* **2007**, *23* (4), 241−256.
(40) Madi, A.; Svinareff, P.; Orange, N.; Feuilloley, M. G. J.; Connil, N. Pseudomonas fluorescens alters epithelial permeability and translocates across Caco-2/TC7 intestinal cells. *Gut Pathog.* **2010**, *2* (1), 16.
(41) Hirakata, Y.; Izumikawa, K.; Yamaguchi, T.; Igimi, S.; Furuya, N.; Maesaki, S.; Tomono, K.; Yamada, Y.; Kohno, S.; Yamaguchi, K.; Kamihira, S. Adherence to and penetration of human intestinal Caco-2 epithelial cell monolayers by Pseudomonas aeruginosa. *Infect. Immun.* **1998**, *66* (4), 1748−1751.
(42) Chauviere, G.; Coconnier, M. H.; Kerneis, S.; Fourniat, J.; Servin, A. L. Adhesion of human Lactobacillus acidophilus strain LB to human enterocyte-like Caco-2 cells. *J. Gen. Microbiol.* **1992**, *138* (Part 8), 1689−1696.
(43) Kerneis, S.; Chauviere, G.; Darfeuille-Michaud, A.; Aubel, D.; Coconnier, M. H.; Joly, B.; Servin, A. L. Expression of receptors for enterotoxigenic Escherichia coli during enterocytic differentiation of human polarized intestinal epithelial cells in culture. *Infect. Immun.* **1992**, *60* (7), 2572−2580.
(44) Grozdanov, L.; Raasch, C.; Schulze, E.; Sonnenborn, U.; Gottschalk, G.; Hacker, J.; Dobrindt, U. Analysis of the genome

structure of the nonpathogenic probiotic Escherichia coli strain Nissle 1917. *J. Bacteriol.* **2004**, *186* (16), 5432−5441.
(45) Bernet, M. F.; Brassart, D.; Neeser, J. R.; Servin, A. L. Lactobacillus acidophilus LA-1 binds to cultured human intestinal cell lines and inhibits cell attachment and cell invasion by enterovirulent bacteria. *Gut* **1994**, *35* (4), 483−489.
(46) Reid, G.; Burton, J. Use of Lactobacillus to prevent infection by pathogenic bacteria. *Microbes Infect.* **2002**, *4* (3), 319−324.
(47) Lee, Y. K.; Puong, K. Y.; Ouwehand, A. C.; Salminen, S. Displacement of bacterial pathogens from mucus and Caco-2 cell surface by lactobacilli. *J. Med. Microbiol.* **2003**, *52* (10), 925−930.
(48) Jankowska, A.; Laubitz, D.; Antushevich, H.; Zabielski, R.; Grzesiuk, E. Competition of Lactobacillus paracasei with Salmonella enterica for adhesion to Caco-2 cells. *J. Biomed. Biotechnol.* **2008**, DOI: 10.1155/2008/357964.
(49) Moussavi, M.; Adams, M. C. An In Vitro Study on Bacterial Growth Interactions and Intestinal Epithelial Cell Adhesion Characteristics of Probiotic Combinations. *Curr. Microbiol.* **2010**, *60* (5), 327−335.
(50) Oelschlaeger, T. A.; Altenhoefer, A.; Hacker, J. Inhibition of Salmonella typhimurium invasion into intestinal cells by the probiotic E. coli strain Nissle 1917. *Gastroenterology* **2001**, *120* (5), A326−A326.
(51) Altenhoefer, A.; Oswald, S.; Sonnenborn, U.; Enders, C.; Schulze, J.; Hacker, J.; Oelschlaeger, T. A. The probiotic Escherichia coli strain Nissle 1917 interferes with invasion of human intestinal epithelial cells by different enteroinvasive bacterial pathogens. *FEMS Immunol. Med. Microbiol.* **2004**, *40* (3), 223−229.
(52) Schierack, P.; Kleta, S.; Tedin, K.; Babila, J. T.; Oswald, S.; Oelschlaeger, T. A.; Hiemann, R.; Paetzold, S.; Wieler, L. H. E. coli Nissle 1917 Affects Salmonella Adhesion to Porcine Intestinal Epithelial Cells. *PLoS One* **2011**, *6* (2), e14712 DOI: 10.1371/journal.pone.0014712.
(53) Brown, E. Probiotic Nissle 1917 shown to reduce Salmonella typhimurium intestinal colonization. *Future Microbiol.* **2013**, *8* (9), 1060−1060.
(54) Silva, M.; Jacobus, N. V.; Deneke, C.; Gorbach, S. L. Antimicrobial substance from a human Lactobacillus strain. *Antimicrob. Agents Chemother.* **1987**, *31* (8), 1231−1233.
(55) Coconnier, M. H.; Lievin, V.; BernetCamard, M. F.; Hudault, S.; Servin, A. L. Antibacterial effect of the adhering human Lactobacillus acidophilus strain LB. *Antimicrob. Agents Chemother.* **1997**, *41* (5), 1046−1052.
(56) Storm, D. W.; Koff, S. A.; Horvath, D. J., Jr.; Li, B.; Justice, S. S. In Vitro Analysis of the Bactericidal Activity of Escherichia Coli Nissle 1917 Against Pediatric Uropathogens. *J. Urol.* **2011**, *186* (4), 1678−1683.